PREPUBLICACIONES DEL DEPARTAMENTO
DE MATEMÁTICA APLICADA
UNIVERSIDAD COMPLUTENSE DE MADRID
MA-UCM 2012-09

Analysis and Simplification of a Mathematical Model for High-Pressure Food Processes

N. A. S. Smith, S. L. Mitchell and A. M. Ramos

Septiembre-2012

http://www.mat.ucm.es/deptos/ma
e-mail:matemática_aplicada@mat.ucm.es

Analysis and Simplification of a Mathematical Model for High-Pressure Food Processes

N. A. S. Smith * S. L. Mitchell † Á. M. Ramos ‡

July 23, 2012

Abstract

Nowadays, consumers look for minimally processed, additive-free food products that maintain their organoleptic properties. This has led to the development of new technologies for food processing. One emerging technology is high hydrostatic pressure, as it proves to be very effective in prolonging the shelf life of foods without losing its properties. Recent research has involved modelling and simulating the effect of combining thermal and high pressure processes (see [3, 5, 6, 9]). The focus is mainly on the inactivation of certain enzymes and microorganisms that are harmful to food. Various mathematical models that study the behaviour of these enzymes and microorganisms during a high pressure process have been proposed (see [5, 6]). Such models need the temperature and pressure profiles of the whole process as an input. In this paper we present two dimensional models, with different kind of boundary conditions, to calculate the temperature profile for solid type foods. We give an exact solution and propose several simplifications, in both two and one dimensions. The temperature profile of these simplified two and one dimensional models is calculated both numerically and analytically, and the solutions are compared. Our results show a very good agreement for all the approximations proposed, and so we can conclude that the simplifications and dimensional reduction are reasonable for certain parameter values, which are specified in this work.

1 Introduction

Classical industrial food conservation processes are based on thermal treatments, such as pasteurization, sterilization and freezing. For classical heat application processes, temperature is in a range of 60 to 120°C, and the processing time can vary from a few seconds to several minutes. The main aim of these processes is to inactivate microorganisms and enzymes that are harmful to food, in order to prolong its shelf life, to maintain or even to improve its natural qualities, and, perhaps most importantly, to provide consumers with products in good a condition. The problem of processing food via thermal treatments is that it may loose a significant part of its nutritional and organoleptic properties. At present, consumers look for minimally processed, additive-free food products that maintain such properties. Therefore the development of new technologies with lower processing temperatures has increased notoriously in the past years (see, e.g., [10, 11]). One of the technologies that can be used in this field is High Pressure (HP) processing, which has turned out to be very effective in inactivating enzymes and microorganisms in food, while leaving small molecules (such as flavor and vitamins) intact, and therefore not modifying significantly the organoleptic properties (see, e.g., [1, 12]).

*Departamento de Matemática Aplicada, Universidad Complutense de Madrid. Corresponding author (nas.smith@mat.ucm.es)

†Mathematics Applications Consortium for Science and Industry (MACSI), Department of Mathematics and Statistics, University of Limerick, Limerick, Ireland.

‡Departamento de Matemática Aplicada, Universidad Complutense de Madrid.

Two principles underlie the effect of HP: firstly, the Le Chatelier Principle, according to which any phenomenon (phase transition, chemical reaction, chemical reactivity, change in molecular configuration) accompanied by a decrease in volume will be enhanced by pressure. Secondly, pressure is instantaneously and uniformly transmitted independently of the size and geometry of the food (isostatic pressure). This uniformity throughout the sample is one of the main advantages of HP when compared to thermal processing. Nevertheless, pressurisation (depressurisation) induces a temperature increase (decrease) due to the work of compression (expansion) inside the food. This change in temperature must be accounted for in a mathematical model. Furthermore, heat exchange between the walls of the pressure chamber, the pressure medium, packaging material and the pressurised food induce a time and space dependent temperature field.

Securing temperature uniformity in HP processed products is crucial for assuring uniform distribution of the pursued pressure effects (e.g. microbial and enzyme inactivation), and the prediction of thermal history within a product under pressure is essential for optimising and homogenising HP process (see Otero *et al.* [10]). For this reason, research has focused (see Otero *et al.* [9]) on heat transfer models that simulate the combination of HP and thermal treatments on food products. Infante *et al.* [5] analyse the temperature distribution and investigate its use as an input for the inactivation of certain enzymes. Both solid- and liquid-type foods are considered. The complexity needed to solve the models (which include heat and mass transfer and non-constant thermo physical properties) can be very high. Knoerzer *et al.* [6] considered a model that predicted flow and temperature fields inside a pilot scale vessel during the pressure heating, holding and cooling stages, again the resulting model was very complex and so difficult to analyse. A numerical model for predicting conductive heat transfer during batch HP processing of foods was developed by Denys *et al.* [3] and tested for a food simile (agar gel). Nonlinear and non-isotropic thermal properties were used, which also led to a complicated numerical scheme. Smith *et al.* [13] presented a generalized enthalpy model for a HP Shift Freezing process based on volume fractions dependent on temperature and pressure.

In this paper we focus only on solid type foods, with a large filling ratio, where convection effects do not need to be taken into account. We perform a dimensional analysis which highlights the dominant terms in the model, and shows that in some cases the equations can be simplified (in dimension) and yet provide a good approximation. These models are much simpler than those found in the literature [3, 5, 6], but still have the correct qualitative features, and hence would be very important when designing suitable industrial equipments and optimizing the processes. Moreover, using the solutions we propose, there is no need to have an FEM solver in order to simulate the process.

In Section 2 we describe the problem and present the governing equations to calculate the temperature distribution. A dimensional analysis is then performed to simplify the model. Sections 3 and 4 contain a thorough investigation of the complete and simplified models for the pressure up and pressure hold times, respectively, and we are able to find exact and approximate solutions describing the whole process. In Section 5 we present some numerical results of a particular process, comparing all the models to exact and numerical solutions. Section 6 briefly considers an extension to third class boundary conditions and, finally, in Section 7 we give concluding remarks.

2 Problem Description

When high pressure is applied in food technology, it is necessary to take into account the thermal effects that are produced by variations of temperature due to the compression/expansion occurring in the food sample and the pressurizing medium. In practice, the pressure evolution, $P(t)$, is known as it is imposed by the user and the limits of the equipment. The temperature of the processed food may change with time and space, therefore we need a heat transfer model capable of predicting the temperature for the processed food. Following [5, 9], a heat transfer model taking into account only conduction effects is presented (for models including convection effects see also [5, 9]). As the model

is both time and spatially dependent, we also introduce a brief description of the domain describing the high pressure device considered in our simulations.

2.1 Mathematical Model

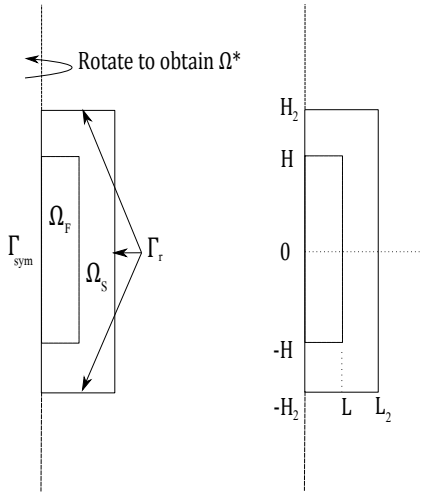

Figure 1: *Computational domain.*

Usually HP experiments on food are carried out in a cylindrical pressure vessel (typically a hollow steel cylinder) that is filled with the food and the pressurizing fluid. It is common to assume axial symmetry (see e.g. [3, 5, 6, 9]), due to the characteristics of this kind of processes, which allows the use of cylindrical coordinates, and to consider a two-dimensional domain with a half cross-section. In this paper we analyse a simplified geometry with only the food and the surrounding steel (see Figure 1). Other authors (see e.g. [5, 9]) have analysed a more complex geometry that also includes the pressurizing fluid and the rubber cap of sample holder, and even the carrier (see [6]). Our focus is on studying a solid type food with a large filling ratio, where the pressure medium represents a low proportion of the vessel content, and so the pressurizing fluid can be ignored.

The domain in the cylindrical (r, z)-coordinates is the rectangle $\Omega = [0, L_2] \times [-H_2, H_2]$ defined by $\overline{\Omega} = \overline{\Omega_{\rm F} \cup \Omega_{\rm S}}$, where $\Omega_{\rm F} = [0, L] \times [-H, H]$ is the food domain, and $\Omega_{\rm S}$ is the domain of the steel that surrounds the food. We use Ω^* to denote the 3D domain generated by rotating Ω along the axis of symmetry ($\{0\} \times (-H_2, H_2)$). The boundary of Ω is denoted by $\Gamma = \Gamma_{\rm r} \cup \Gamma_{\rm sym}$, where we can distinguish $\Gamma_{\rm r}$ on which the temperature is known, and $\Gamma_{\rm sym}$ that has zero heat flux by axial symmetry.

For the mathematical modelling two significantly different cases can be studied: solid and liquid type foods. Since we are only concerned in analysing solid type foods with a large filling ratio, we only take into account conduction effects (and neglect convection effects). This simplification has been shown to lead to quite accurate results (see [5, 9]). Thus, when solid type foods are considered, we start with the heat conduction equation for temperature T (K)

$$\rho C_p \frac{\partial T}{\partial t} - \nabla \cdot (k \nabla T) = \beta \, \frac{{\rm d}P}{{\rm d}t} \, T \qquad \text{in} \quad \Omega^* \times (0, t_{\rm f}), \tag{1}$$

where ρ is the density (kg m^{-3}), C_p the specific heat (J kg^{-1} K^{-1}), k the thermal conductivity (W m^{-1} K^{-1}) and $t_{\rm f}$ is the final time (s). The right hand side of equation (1) is the heat production due to the change of pressure $P = P(t)$ (Pa) applied by the equipment (chosen by the user within the

machine limitations) and β is the thermal expansion coefficient defined by

$$\beta = \begin{cases} \beta_{\mathrm{F}}: \text{ thermal expansion coefficient } (\mathrm{K}^{-1}) \text{ of the food in } \Omega_{\mathrm{F}}^{*}, \\ 0, \text{ in the steel domain.} \end{cases}$$

This term results from the following law (see [6])

$$\frac{\Delta T}{\Delta P} = \frac{\beta T V}{M C_p} = \frac{\beta T}{\rho C_p}, \tag{2}$$

where ΔT denotes the temperature change due to the pressure change ΔP, V is the volume and M the mass.

By using cylindrical coordinates and taking into account axial symmetry, equation (1) may be re-written in 2D as

$$\rho\, C_p\, \frac{\partial T}{\partial t} - \frac{1}{r}\frac{\partial}{\partial r}\left(rk\frac{\partial T}{\partial r}\right) - \frac{\partial}{\partial z}\left(k\frac{\partial T}{\partial z}\right) = \beta\, \frac{\mathrm{d}P}{\mathrm{d}t}\, T \qquad \text{in} \quad \Omega \times (0, t_{\mathrm{f}}). \tag{3}$$

Equation (3) must be completed with appropriate boundary and initial conditions depending on the HP machine and the problem we wish to solve. For simplicity we assume that the outer walls of the domain are kept at a constant temperature T_{r}, and that the initial temperature T_0 is constant in each region, therefore giving

$$\begin{cases} \dfrac{\partial T}{\partial r} = 0 & \text{on} \quad \Gamma_{\mathrm{sym}}, \\ T = T_{\mathrm{r}} & \text{on} \quad \Gamma_{\mathrm{r}}, \\ T = T_0 & \text{at} \quad t = 0. \end{cases} \tag{4}$$

In Section 6 we briefly discuss an extended model with third class boundary conditions. Several authors have considered different boundary conditions to those described above. Infante *et al.* [5] and Otero *et al.* [9] assumed a boundary was kept at a refrigerated temperature, as well as a boundary allowing for heat transfer with the room. Denys *et al.* [3] considered an overall heat transfer coefficient at the surface of the cylinder to account for heat transfer through the walls of the HP vessel. Although our conditions (4) may seem overly simplistic from a practical consideration, it has been suggested in the literature that keeping the walls of machine at a constant temperature may be good for avoiding heat loss [10]. There can be a problem of heat loss through the wall of the high-pressure vessel, and by anticipating the temperature increase of the processed product, resulting from compression, conductive heat transfer and temperature gradients can be avoided [3].

In the following sections we study exact and approximate solutions for the model with first class boundary conditions. It is convenient to begin by non-dimensionalising the model to highlight whether any simplifications are possible.

2.2 Dimensional analysis

Given that the pressure function in equation (3) only appears in a derivative form, and that the pressure applied on these processes is typically a piecewise linear function in time (hence such a derivative is usually piecewise constant) we do not non-dimensionalise the pressure variable. Instead, we rewrite the pressure derivative $\frac{\mathrm{d}P}{\mathrm{d}t}(t)$ as

$$\frac{\mathrm{d}P}{\mathrm{d}t}(t) = \begin{cases} \dfrac{\gamma}{t_{\mathrm{p}}}, & 0 < t \leq t_{\mathrm{p}}, \\ 0, & t > t_{\mathrm{p}}, \end{cases} \tag{5}$$

where, for the sake of simplicity, we suppose that $\frac{\mathrm{d}P}{\mathrm{d}t}(t) = \frac{\gamma}{t_\mathrm{p}} > 0$ (P linear) for all $t \in [0, t_\mathrm{p}]$, and γ (Pa) is the maximum pressure reached (for the sake of simplicity we assume that atmospheric pressure is 0 MPa, instead of 0.1 MPa, which is typically the real value). After time t_p the pressure is maintained constant at the maximum value, and therefore the derivative is zero (other cases can be also studied similarly). The release of pressure that takes place after t_f can be modelled with the same approach. Since it does not introduce any further difficulty we have not considered it here.

Therefore, for $0 < t \leq t_\mathrm{p}$ equation (3) can be written as

$$\rho\ C_p\ \frac{\partial T}{\partial t} - \frac{1}{r}\frac{\partial}{\partial r}\left(rk\frac{\partial T}{\partial r}\right) - \frac{\partial}{\partial z}\left(k\frac{\partial T}{\partial z}\right) = \beta\ \frac{\gamma}{t_\mathrm{p}}\ T, \tag{6}$$

and for $t_\mathrm{p} < t \leq t_\mathrm{f}$ the same equation holds, except with the right-hand side equal to zero.

The system is now non-dimensionalised by setting

$$\hat{r} = \frac{r}{R}, \qquad \hat{z} = \frac{z}{Z}, \qquad \hat{t} = \frac{t}{\tau}, \qquad \hat{T} = \frac{T - T_\mathrm{r}}{\Delta T},$$

where ΔT, R, Z and τ are suitable temperature, radius, height and time scales, respectively.

Thus, for $0 < \hat{t} \leq \frac{t_\mathrm{p}}{\tau}$, equation (6) becomes

$$\frac{\rho\ C_p\ \Delta T}{\tau}\frac{\partial \hat{T}}{\partial \hat{t}} - \frac{k\Delta T}{R^2\hat{r}}\frac{\partial}{\partial \hat{r}}\left(\hat{r}\frac{\partial \hat{T}}{\partial \hat{r}}\right) - \frac{k\Delta T}{Z^2}\frac{\partial^2 \hat{T}}{\partial \hat{z}^2} = \frac{\beta\gamma\Delta T}{t_\mathrm{p}}(\hat{T} + \frac{T_\mathrm{r}}{\Delta T}). \tag{7}$$

For ease of notation we drop the $\hat{}$ notation, and so T, z, r and t are now the non-dimensional variables.

We divide equation (7) by $\rho C_p \Delta T/\tau$, resulting in

$$\frac{\partial T}{\partial t} - \frac{k\tau}{R^2\rho C_p}\frac{1}{r}\frac{\partial}{\partial r}\left(r\frac{\partial T}{\partial r}\right) - \frac{k\tau}{Z^2\rho C_p}\frac{\partial^2 T}{\partial z^2} = \frac{\beta\gamma\tau}{\rho C_p t_\mathrm{p}}T + \frac{\beta\gamma\tau}{\rho C_p t_\mathrm{p}}\frac{T_\mathrm{r}}{\Delta T}. \tag{8}$$

The dimensionless groups of parameters in equation (8) are

$$a = \frac{k\tau}{R^2\rho C_p}, \qquad b = \frac{k\tau}{Z^2\rho C_p}, \qquad c = \frac{\beta\gamma\tau}{\rho C_p t_\mathrm{p}}, \qquad d = \frac{\beta\gamma\tau}{\rho C_p t_\mathrm{p}}\frac{T_\mathrm{r}}{\Delta T}. \tag{9}$$

The radius and height scales that we propose come from the dimensions of the food cylinder, giving $R = L$ and $Z = H$. Note that we are only considering half of the height of the domain as the z scale for the sake of simplicity. For the temperature scale we set $\Delta T = \max\{|T_0 - T_\mathrm{r}|, \frac{\beta\gamma T_0}{\rho C_p}\}$, where ρ and C_p are the density and specific heat of the food sample, respectively. The quantity $\frac{\beta\gamma T_0}{\rho C_p}$ is the maximum increase of temperature in the food sample due to the increase of pressure (according to (2)). The time scale τ is chosen from equation (8). We wish to investigate what happens when the pressure is increased and therefore balance the pressure term with the time derivative. This leads to

$$\tau = \frac{\rho C_p t_\mathrm{p}}{\beta\gamma}\min\ \left\{1, \frac{\Delta T}{T_\mathrm{r}}\right\}.$$

The system in non-dimensional form is therefore given by

$$\begin{cases} \dfrac{\partial T}{\partial t} - a\dfrac{1}{r}\dfrac{\partial}{\partial r}\left(r\dfrac{\partial T}{\partial r}\right) - b\dfrac{\partial^2 T}{\partial z^2} = (cT + d)\chi(t) & \text{in} \quad \hat{\Omega} \times (0, t_\mathrm{f}), \\ \dfrac{\partial T}{\partial r} = 0 & \text{on} \quad \hat{\Gamma}_{\mathrm{sym}}, \\ T = 0 & \text{on} \quad \hat{\Gamma}_\mathrm{r}, \\ T = T_0^* & \text{at} \quad t = 0, \end{cases} \tag{10}$$

where $\hat{\Omega} = (0, \frac{L_2}{L}) \times (\frac{-H_2}{H}, \frac{H_2}{H})$ is the non-dimensional form of the whole domain Ω. The function $\chi(t)$ is defined as

$$\chi(t) = \begin{cases} 1, & \text{if } \ t \in (0, t_{\rm p}), \\ 0, & \text{elsewhere.} \end{cases}$$

Note that $t_{\rm p}/\tau$ and $t_{\rm f}/\tau$ have been redefined as $t_{\rm p}$ and $t_{\rm f}$ for convenience. The non-dimensional initial value is

$$T_0^* = \frac{T_0 - T_{\rm r}}{\Delta T}. \tag{11}$$

It should be pointed out that in (9), $b = a\frac{R^2}{Z^2}$ and hence with the chosen scales $b = a\frac{L^2}{H^2}$. This will mean that if the food sample holder is narrow and tall (which is usually the case for the HP pilot scale machines), the conduction parameter in the z direction, b, will be smaller than that in the r direction, a. Thus we wish to investigate whether the heat transfer due to conduction is dominant in the radial direction over the height direction, for a thin and tall machine. This will be studied in Sections 3.2 and 4.2.

System (10) is set in $\hat{\Omega}$, which involves the two regions to determine the temperature in the food, $T_{\rm F}$, and in the steel, $T_{\rm S}$. Taking into account that parameters c and d defined in (9) are zero in the steel region, as $\beta = 0$, (10) is defined as

$$\begin{cases} \dfrac{\partial T_{\rm F}}{\partial t} - a_{\rm F}\dfrac{1}{r}\dfrac{\partial}{\partial r}\left(r\dfrac{\partial T_{\rm F}}{\partial r}\right) - b_{\rm F}\dfrac{\partial^2 T_{\rm F}}{\partial z^2} = (c_{\rm F}T_{\rm F} + d_{\rm F})\chi(t) & \text{in} \quad \hat{\Omega}_{\rm F} \times (0, t_{\rm f}), \\ \dfrac{\partial T_{\rm S}}{\partial t} - a_{\rm S}\dfrac{1}{r}\dfrac{\partial}{\partial r}\left(r\dfrac{\partial T_{\rm F}}{\partial r}\right) - b_{\rm S}\dfrac{\partial^2 T_{\rm S}}{\partial z^2} = 0 & \text{in} \quad \hat{\Omega}_{\rm S} \times (0, t_{\rm f}), \\ \dfrac{\partial T_{\rm F}}{\partial r} = 0, \qquad \dfrac{\partial T_{\rm S}}{\partial r} = 0 & \text{on} \quad \hat{\Gamma}_{\rm sym}, \\ k_{\rm F}\dfrac{\partial T_{\rm F}}{\partial r} = k_{\rm S}\dfrac{\partial T_{\rm S}}{\partial r}, \qquad T_{\rm F} = T_{\rm S} & \text{on} \quad \hat{\Gamma}_{\rm FS}, \\ T_{\rm S} = 0 & \text{on} \quad \hat{\Gamma}_{\rm r}, \\ T_{\rm F} = T_{\rm F_0}^*, \qquad T_{\rm S} = T_{\rm S_0}^* & \text{at} \quad t = 0, \end{cases} \tag{12}$$

where $T_{\rm F_0}^*$ and $T_{\rm S_0}^*$ are the non-dimensional initial temperatures in the food and steel, respectively. $\hat{\Omega}_{\rm F} = (0, 1) \times (-1, 1)$ is the non-dimensional food region, and $\hat{\Omega}_{\rm S} = \hat{\Omega} - \hat{\Omega}_{\rm F}$ the steel one. On the non-dimensional food-steel boundary, $\hat{\Gamma}_{\rm FS} = \big[(0, 1) \times \{1\}\big] \cup \big[(0, 1) \times \{-1\}\big] \cup \big[\{1\} \times (-1, 1)\big]$, continuity of the solution and the fluxes has been imposed.

We begin by determining an approximate solution for the steel temperature. By assuming that the conductivity of steel is much larger than that of the food, we can simplify the flux boundary condition on $\hat{\Gamma}_{\rm FS}$

$$\frac{\partial T_{\rm S}}{\partial r} = \frac{k_{\rm F}}{k_{\rm S}}\frac{\partial T_{\rm F}}{\partial r} \approx 0, \qquad \text{on } \hat{\Gamma}_{\rm FS}. \tag{13}$$

If we also assume that we are working with a narrow and tall machine, i.e. that $L << H$, and hence $b_{\rm S} << a_{\rm S}$, the equation for the steel reduces to

$$\frac{\partial T_{\rm S}}{\partial t} - a_{\rm S}\frac{1}{r}\frac{\partial}{\partial r}\left(r\frac{\partial T_{\rm F}}{\partial r}\right) = 0, \qquad \text{in } \hat{\Omega}_{\rm S} \times (0, t_{\rm f}). \tag{14}$$

Since steel has a high thermal diffusivity, $a_{\rm S}$, the solution of (14) goes to steady state very rapidly, and the solution to the steady state problem is zero (using the zero flux and zero temperature boundary conditions). Hence we can conclude that $T_{\rm S} \approx 0$. Then the boundary condition for the food at $\hat{\Gamma}_{\rm FS}$ can be approximated by $T_{\rm F} \approx 0$.

Thus, we now only have the temperature in the food problem to solve, and (12) reduces to

$$\begin{cases} \dfrac{\partial T_{\mathrm{F}}}{\partial t} - a_{\mathrm{F}}\dfrac{1}{r}\dfrac{\partial}{\partial r}\left(r\dfrac{\partial T_{\mathrm{F}}}{\partial r}\right) - b_{\mathrm{F}}\dfrac{\partial^2 T_{\mathrm{F}}}{\partial z^2} = (c_{\mathrm{F}}T_{\mathrm{F}} + d_{\mathrm{F}})\chi(t) & \text{in} \quad (0,1)\times(-1,1)\times(0,t_{\mathrm{f}}), \\ \dfrac{\partial T_{\mathrm{F}}}{\partial r} = 0 & \text{on} \quad r = 0, \\ T_{\mathrm{F}} = 0 & \text{on} \quad r = 1, \\ T_{\mathrm{F}} = 0 & \text{on} \quad z = -1, \\ T_{\mathrm{F}} = 0 & \text{on} \quad z = 1, \\ T_{\mathrm{F}} = T^*_{\mathrm{F}_0} & \text{at} \quad t = 0. \end{cases} \tag{15}$$

One further simplification of system (15) can be made, and this is to divide the domain in half at $z = 0$ and impose a zero flux boundary condition. Due to symmetry we only need to solve the problem in the upper half of the domain. Finally we have system for T_{F} (that we will simply refer to as T henceforth)

$$\begin{cases} \dfrac{\partial T}{\partial t} - a\dfrac{1}{r}\dfrac{\partial}{\partial r}\left(r\dfrac{\partial T}{\partial r}\right) - b\dfrac{\partial^2 T}{\partial z^2} = (cT + d)\chi(t) & \text{in} \quad (0,1)\times(0,1)\times(0,t_{\mathrm{f}}), \\ \dfrac{\partial T}{\partial r} = 0 & \text{on} \quad r = 0, \\ T = 0 & \text{on} \quad r = 1, \\ \dfrac{\partial T}{\partial z} = 0 & \text{on} \quad z = 0, \\ T = 0 & \text{on} \quad z = 1, \\ T = T^*_0 & \text{at} \quad t = 0. \end{cases} \tag{16}$$

3 Analysis for the pressure up time $0 \le t \le t_{\mathrm{p}}$

3.1 Exact solution

An exact solution can be found by solving the 2D system (16) using separation of variables. We can create a homogeneous problem by setting

$$T(r,z,t) = u(r,z,t) + v(r,z) + w(z). \tag{17}$$

Then the problem to solve for u is

$$\begin{cases} \dfrac{\partial u}{\partial t} = a\dfrac{1}{r}\dfrac{\partial}{\partial r}\left(r\dfrac{\partial u}{\partial r}\right) + b\dfrac{\partial^2 u}{\partial z^2} + cu & \text{in} \quad (0,1)\times(0,1)\times(0,t_{\mathrm{p}}), \\ \dfrac{\partial u}{\partial r} = 0 & \text{on} \quad r = 0, \\ u = 0 & \text{on} \quad r = 1, \\ \dfrac{\partial u}{\partial z} = 0 & \text{on} \quad z = 0, \\ u = 0 & \text{on} \quad z = 1, \\ u = T^*_0 - v(r,z) - w(z) & \text{at} \quad t = 0, \end{cases} \tag{18}$$

whilst the problem for v is

$$\begin{cases} 0 = a\dfrac{1}{r}\dfrac{\partial}{\partial r}\left(r\dfrac{\partial v}{\partial r}\right) + b\dfrac{\partial^2 v}{\partial z^2} + cv & \text{in} \quad (0,1)\times(0,1)\times(0,t_{\mathrm{p}}), \\ \dfrac{\partial v}{\partial r} = 0 & \text{on} \quad r = 0, \\ v = -w(z) & \text{on} \quad r = 1, \\ \dfrac{\partial v}{\partial z} = 0 & \text{on} \quad z = 0, \\ v = 0 & \text{on} \quad z = 1, \end{cases} \tag{19}$$

and the problem for w is

$$bw''(z) + cw(z) + d = 0, \qquad w'(0) = 0, \qquad w(1) = 0. \tag{20}$$

This has solution

$$w(z) = \frac{d}{c}\left(\frac{\cos(\mu z)}{\cos\mu} - 1\right), \tag{21}$$

where $\mu = \sqrt{c/b}$.

We use the method of separation of variables and set $v(r,z) = R(r)Z(z)$. Then the boundary conditions imply that $R'(0) = Z'(0) = Z(1) = 0$. From (19) we deduce that

$$\frac{\frac{a}{r}(R'(r) + rR''(r)) + cR(r)}{bR(r)} = -\frac{Z''(z)}{Z(z)} = \nu^2, \tag{22}$$

for suitable constants $\nu \in \mathbb{R}$, where $(\cdot)'$ denotes differentiation with respect to each variable. Solving the ODE for $Z(z)$ leads to

$$Z_p(z) = A_{Zp}\cos(\nu_p z), \qquad p = 1,\, 2,\, \ldots, \tag{23}$$

with $A_{Zp} \in \mathbb{R}$, and $\nu_p = (p - 1/2)\pi$. The solution of the ODE for $R(r)$, after satisfying the boundary condition $R'(0) = 0$, is

$$R_p(r) = A_{Rp}J_0(\alpha_p r), \tag{24}$$

where J_n is the Bessel function of the first kind of order n, $A_{Rp} \in \mathbb{R}$, and

$$\alpha_p = \sqrt{\frac{c - \nu_p^2 b}{a}}. \tag{25}$$

Hence we write

$$v(r,z) = \sum_{p=1}^{\infty} A_p J_0(\alpha_p r)\cos(\nu_p z), \tag{26}$$

and from integrating and applying the orthogonality condition it follows that

$$A_p = -\frac{2}{J_0(\alpha_p)}\int_0^1 w(z)\cos(\nu_p z)\,\mathrm{d}z, \tag{27}$$

where $w(z)$ is defined in (21).

We finally turn to the problem for u in (18) and separate variables by setting $u(r,z,t) = R(r)Z(z)\Gamma(t)$. Then the boundary conditions imply that $R'(0) = R(1) = Z'(0) = Z(1) = 0$. From (18) we deduce that now

$$\frac{\Gamma'(t)}{\Gamma(t)} = \frac{\frac{a}{r}(R'(r) + rR''(r))Z(z) + bR(r)Z''(z) + cR(r)Z(z)}{R(r)Z(z)} = -\lambda^2. \tag{28}$$

and so the first equation is solved to give $\Gamma(t) = B\exp(-\lambda^2 t)$, for suitable constants $\lambda \in \mathbb{R}$. The solutions of R and Z are found in an identical manner to that described above, and so

$$Z_m(z) = C_{Zm}\cos(\nu_m z), \quad m = 1,\, 2,\, \ldots, \qquad R_n(r) = C_{Rn}J_0(\delta_n r), \quad n = 1,\, 2,\, \ldots, \tag{29}$$

where $\nu_m = (m - 1/2)\pi$ and

$$\delta_n = \sqrt{\frac{c + \lambda_{mn}^2 - \nu_m^2 b}{a}}. \tag{30}$$

These are found by solving $J_0(\delta_n) = 0$, in order to satisfy $R(0) = 0$, and then λ_{mn} can be determined from the formula $\lambda_{mn} = \sqrt{a\delta_n^2 + b\nu_m^2 - c}$.

The combined solution for u is therefore

$$u(r,z,t) = \sum_{n=1}^{\infty}\sum_{m=1}^{\infty} D_{mn}J_0(\delta_n r)\cos(\nu_m z)\exp(-\lambda_{mn}^2 t), \tag{31}$$

and coefficients D_{mn} are found using the initial condition in (18). Thus

$$T_0^* - v(r,z) - w(z) = \sum_{n=1}^{\infty}\sum_{m=1}^{\infty} D_{mn}J_0(\delta_n r)\cos(\nu_m z), \tag{32}$$

where $w(z)$ and $v(r,z)$ are defined in (21) and (26)-(27) respectively. Integrating with respect to r and z and using the orthogonality conditions leads to

$$D_{mn} = \frac{2\int_0^1\int_0^1 \left(T_0^* - v(r,z) - w(z)\right)\, rJ_0(\delta_n r)\cos(\nu_m z)\,\mathrm{d}r\,\mathrm{d}z}{\int_0^1 rJ_0^2(\delta_n r)\,\mathrm{d}r}. \tag{33}$$

The solutions for u, v and w are then added together to give the final solution for T in (17).

3.2 Approximation ignoring the z-dependence

If we assume that we are modelling a narrow and tall machine, and hence $b \ll a$, it is reasonable to ignore the z dependence in (16) and solve the 1D problem, which is therefore given by

$$\begin{cases} \dfrac{\partial T}{\partial t} - a\dfrac{1}{r}\dfrac{\partial}{\partial r}\left(r\dfrac{\partial T}{\partial r}\right) = (cT + d) & \text{in} \quad (0,1)\times(0,t_{\mathrm{p}}), \\ \dfrac{\partial T}{\partial r} = 0 & \text{on} \quad r = 0, \\ T = 0 & \text{on} \quad r = 1, \\ T = T_0^* & \text{at} \quad t = 0. \end{cases} \tag{34}$$

We now consider various exact and approximate solutions to this simplified system.

3.2.1 Separation of variables solution

A separation of variables solution to system (34) can be found following the analysis given in Section 3.1. To create a homogeneous problem we substitute $T(r,t) = u(r,t) + v(r)$ into (34). Then the problem to solve for u is

$$\begin{cases} \dfrac{\partial u}{\partial t} = a\dfrac{1}{r}\dfrac{\partial}{\partial r}\left(r\dfrac{\partial u}{\partial r}\right) + cu & \text{in} \quad (0,1)\times(0,t_{\mathrm{p}}), \\ \dfrac{\partial u}{\partial r} = 0 & \text{on} \quad r = 0, \\ u = 0 & \text{on} \quad r = 1, \\ u = T_0^* - v(r) & \text{at} \quad t = 0, \end{cases} \tag{35}$$

whilst the problem for v is

$$0 = \frac{a}{r}\big(v'(r) + rv''(r)\big) + cv + d, \tag{36}$$

with $v'(0) = 0$ and $v(1) = 0$. This has solution

$$v(r) = -\frac{d}{c} + \frac{dJ_0(\sqrt{\frac{c}{a}}r)}{cJ_0(\sqrt{\frac{c}{a}})}. \tag{37}$$

Following the procedure in Section 3.1 a straightforward calculation gives the solution for u as

$$u(r,t) = \sum_{n=1}^{\infty} \bar{D}_n J_0(\bar{\delta}_n r)\exp(-\bar{\lambda}_n^2 t), \tag{38}$$

where $\bar{\delta}_n \in \mathbb{R}$ satisfy $J_0(\bar{\delta}_n) = 0$, $\bar{\lambda}_n = \sqrt{a\bar{\delta}_n^2 - c}$, and coefficients $\bar{D}_n$ are given by

$$\bar{D}_n = \frac{2\int_0^1 \left(T_0^* - v(r)\right)\, rJ_0(\bar{\delta}_n r)\,\mathrm{d}r}{\int_0^1 rJ_0^2(\bar{\delta}_n r)\,\mathrm{d}r}, \tag{39}$$

with $v(r)$ defined in (37). Finally, the solution T is simply the sum of u and v.

3.2.2 Boundary layer solution

Again the starting point is system (34). Let us assume that, as is true for some practical cases (an example of which will be shown in Section 5), $d = \mathcal{O}(1)$ and $b < a \ll 1$. Then ignoring the terms involving a and b, we find

$$\frac{\partial T}{\partial t} = cT + d \tag{40}$$

$$T(0) = T_0^*, \tag{41}$$

which gives the leading order solution

$$T(t) = -\frac{d}{c} + \left(T_0^* + \frac{d}{c}\right)\exp(ct). \tag{42}$$

Note that since solution (42) only depends on t it does satisfy the zero flux condition at $r = 0$, but it obviously cannot satisfy the zero temperature condition at $r = 1$. Thus we assume that (42) is an *outer* solution, $T \equiv T_{\mathrm{out}}(t)$, and that there is a boundary layer at $r = 1$. In this region different

terms will form the dominant balance and so to highlight this we re-scale the problem by introducing a boundary-layer coordinate as

$$\bar{r} = \frac{1-r}{\delta}, \tag{43}$$

where $\delta \ll 1$ is to be determined. This change of variables has the effect of stretching the region near $r = 1$ when $\delta \to 0$, which in practice means that the boundary-layer problem (also known as inner problem) is solved on a infinite domain. If we let $T_{\text{in}}(\bar{r}, t)$ denote the solution of the problem when using the boundary-layer coordinate, then near $r = 1$ the PDE in (34) becomes

$$\frac{\partial T_{\text{in}}}{\partial t} + \frac{a}{\delta}\frac{1}{1-\delta\bar{r}}\frac{\partial T_{\text{in}}}{\partial \bar{r}} - \frac{a}{\delta^2}\frac{\partial^2 T_{\text{in}}}{\partial \bar{r}^2} = cT_{\text{in}} + d. \tag{44}$$

To bring out the correct balance in the equation, we take $\delta = \sqrt{a}$, and so coupled with boundary and initial conditions the leading order problem is

$$\begin{cases} \dfrac{\partial T_{\text{in}}}{\partial t} = \dfrac{\partial^2 T_{\text{in}}}{\partial \bar{r}^2} - \sqrt{a}\dfrac{\partial T_{\text{in}}}{\partial \bar{r}} + cT_{\text{in}} + d & \text{in} \quad (0,\infty)\times(0,t_{\text{p}}), \\ T_{\text{in}} = 0 & \text{on} \quad \bar{r} = 0, \\ T_{\text{in}} \to T_{\text{out}}(t) & \text{as} \quad \bar{r} \to \infty, \\ T_{\text{in}} = T_0^* & \text{at} \quad t = 0, \end{cases} \tag{45}$$

where $T_{\text{out}}(t)$ is the outer solution given in (42). For convenience we subtract off the outer solution to give a new variable which decays to zero as $\bar{r} \to \infty$. Thus, if we define

$$T_{\text{in}}(\bar{r}, t) = T_{\text{out}}(t) + F(\bar{r}, t), \tag{46}$$

the system to solve for F reduces to

$$\begin{cases} \dfrac{\partial F}{\partial t} = \dfrac{\partial^2 F}{\partial \bar{r}^2} - \sqrt{a}\dfrac{\partial F}{\partial \bar{r}} + cF & \text{in} \quad (0,\infty)\times(0,t_{\text{p}}), \\ F = -T_{\text{out}}(t) & \text{on} \quad \bar{r} = 0, \\ F \to 0 & \text{as} \quad \bar{r} \to \infty, \\ F = 0 & \text{at} \quad t = 0. \end{cases} \tag{47}$$

It is first convenient to transform the PDE in (47) into a standard heat equation by setting

$$F(\bar{r}, t) = \exp\left(\frac{\sqrt{a}\,\bar{r}}{2} + ct - \frac{at}{4}\right) G(\bar{r}, t). \tag{48}$$

Then (47) becomes

$$\begin{cases} \dfrac{\partial G}{\partial t} = \dfrac{\partial^2 G}{\partial \bar{r}^2} & \text{in} \quad (0,\infty)\times(0,t_{\text{p}}), \\ G = -T_{\text{out}}(t)\exp(-ct + \frac{at}{4}) & \text{on} \quad \bar{r} = 0, \\ G \to 0 & \text{as} \quad \bar{r} \to \infty, \\ G = 0 & \text{at} \quad t = 0. \end{cases} \tag{49}$$

At first glance it appears that this system can be solved using Laplace transforms. However, the resulting transformed solution is not easy to invert using standard tables and so the solution would have to be given as a complex integral. To avoid this we instead use Fourier sine transforms, which is appropriate because there is a fixed boundary condition at $\bar{r} = 0$. Given a function $f(x)$, $0 \le x < \infty$, the Fourier sine transform pair is defined as

$$\hat{f}(\omega) = \frac{2}{\pi}\int_0^\infty f(x)\sin(\omega x)\,\mathrm{d}x, \qquad f(x) = \int_0^\infty \hat{f}(\omega)\sin(\omega x)\,\mathrm{d}\omega. \tag{50}$$

Now if

$$\hat{G}(\omega, t) = \frac{2}{\pi}\int_0^\infty G(\bar{r}, t)\sin(\omega\bar{r})\,\mathrm{d}\bar{r}, \tag{51}$$

then the PDE in (49) becomes

$$\frac{\partial \hat{G}}{\partial t} + \omega^2\hat{G} = -\frac{2\omega T_{\mathrm{out}}(t)\exp\left(\frac{at}{4} - ct\right)}{\pi}. \tag{52}$$

Note that when differentiating $\hat{G}$ with respect to r twice, we have used the additional condition $\frac{\partial G}{\partial \bar{r}} \to 0$ as $\bar{r} \to \infty$, which follows from matching with the outer solution, that only depends on t.

The initial condition in (49) implies that $\hat{G}(\omega, 0) = 0$ and so equation (52) has solution

$$\hat{G}(\omega, t) = \frac{2\omega d}{\pi c(\omega^2 + a/4 - c)}\big[\exp(at/4 - ct) - \exp(-\omega^2 t)\big] - \frac{2\omega(T_0^* + d/c)}{\pi(\omega^2 + a/4)}\big[\exp(at/4) - \exp(-\omega^2 t)\big], \tag{53}$$

after substituting $T_{\mathrm{out}}(t)$ from (42). Finally the solution for G is given by

$$G(\bar{r}, t) = \int_0^\infty \hat{G}(\omega, t)\sin(\omega\bar{r})\,\mathrm{d}\omega, \tag{54}$$

and so

$$T_{\mathrm{in}}(\bar{r}, t) = T_{\mathrm{out}}(t) + \exp\left(\frac{\sqrt{a}\,\bar{r}}{2} - \frac{at}{4} + ct\right)G(\bar{r}, t). \tag{55}$$

After adding the inner and outer solutions and subtracting the common part, we can write down the final solution in the whole domain as

$$T(r, t) = -\frac{d}{c} + \left(T_0^* + \frac{d}{c}\right)\exp(ct) + \exp\left(\frac{1 - r}{2} + ct - \frac{at}{4}\right)G\left(\frac{1 - r}{\sqrt{a}}, t\right). \tag{56}$$

3.3 Approximation including the z-dependence

Since the approximate solutions in Section 3.2 only depend on r and t it is clear that the boundary condition at $z = 1$ is not satisfied (unlike the zero flux boundary condition at $z = 0$, which is satisfied). We need to consider a boundary layer analysis near $z = 1$, and therefore follow a similar analysis to that given in Section 3.2.2. Thus we set $z = 1 - \sqrt{b}\bar{z}$ and denote $T_{\mathrm{in}}(r, \bar{z}, t)$ as the inner solution. Then, for leading order terms, system (16) becomes

$$\begin{cases} \dfrac{\partial T_{\mathrm{in}}}{\partial t} - a\dfrac{1}{r}\dfrac{\partial}{\partial r}\left(r\dfrac{\partial T_{\mathrm{in}}}{\partial r}\right) - \dfrac{\partial^2 T_{\mathrm{in}}}{\partial \bar{z}^2} = (cT_{\mathrm{in}} + d) & \text{in} \quad (0,1)\times(0,\infty)\times(0,t_{\mathrm{p}}), \\ \dfrac{\partial T_{\mathrm{in}}}{\partial r} = 0 & \text{on} \quad r = 0, \\ T_{\mathrm{in}} = 0 & \text{on} \quad r = 1, \\ T_{\mathrm{in}} \to T_{\mathrm{out}} & \text{as} \quad \bar{z} \to \infty, \\ T_{\mathrm{in}} = 0 & \text{on} \quad \bar{z} = 0, \\ T_{\mathrm{in}} = T_0^* & \text{at} \quad t = 0, \end{cases} \tag{57}$$

where T_{out} is the outer solution of the PDE, i.e. the solution that we solved in Section 3.2. We will use the series solution found in Section 3.2.1, namely

$$T_{\text{out}}(r,t) = v(r) + \sum_{n=1}^{\infty} \bar{D}_n J_0(\bar{\delta}_n r) \exp(-\bar{\lambda}_n^2 t), \tag{58}$$

where $v(r)$ is given in (37). Whilst we could use the boundary layer solution (56), this form is simpler as it avoids a solution involving several integrals.

Using the same approach as in Section 3.2.2, if we set

$$T_{\text{in}}(r,\bar{z},t) = T_{\text{out}}(r,t) + F(r,\bar{z},t), \tag{59}$$

then the PDE in (57) becomes

$$\frac{\partial F}{\partial t} = a\frac{1}{r}\frac{\partial}{\partial r}\left(r\frac{\partial F}{\partial r}\right) + \frac{\partial^2 F}{\partial \bar{z}^2} + cF, \tag{60}$$

which follows since $T_{\text{out}}(r,t)$ satisfies the outer PDE. If, as at the start of Section 3.2.2, we assume $a \ll 1$ and then ignore this term here, system (57) reduces to the following 1D problem:

$$\begin{cases} \dfrac{\partial F}{\partial t} - \dfrac{\partial^2 F}{\partial \bar{z}^2} = cF & \text{in} \quad (0,\infty)\times(0,t_{\text{p}}), \\ F \to 0 & \text{as} \quad \bar{z}\to\infty, \\ F = h(t) & \text{on} \quad \bar{z}=0, \\ F = 0 & \text{at} \quad t=0, \end{cases} \tag{61}$$

where for convenience we have defined $h(t) = -T_{\text{out}}(r,t)$ (considering r as a constant value and the solving the system for each r). Again using Fourier sine transforms we can find the exact solution to (61). This is given by

$$F(\bar{z},t) = \int_0^{\infty} \left(\frac{2}{\pi}\int_0^t h(t')\exp((\omega^2 - c)(t'-t))\,\mathrm{d}t'\right)\sin(\omega\bar{z})\,\mathrm{d}\omega, \tag{62}$$

or

$$F(\bar{z},t) = \int_0^{\infty} (f_1(\omega,t) + f_2(\omega,t))\sin(\omega\bar{z})\,\mathrm{d}\omega, \tag{63}$$

where

$$f_1(\omega,t) = -\frac{2\omega v(r)}{\pi(c-\omega^2)}\big[\exp((c-\omega^2)t) - 1\big], \tag{64}$$

$$f_2(\omega,t) = \frac{2}{\pi}\sum_{n=0}^{\infty} \bar{D}_n J_0(\bar{\delta}_n r)\frac{\big[\exp(-\bar{\lambda}_n^2 t) - \exp((c-\omega^2)t)\big]}{\bar{\lambda}_n^2 + c - \omega^2}. \tag{65}$$

Thus, the inner solution is simply the sum of F and T_{out}. After adding the inner and outer solutions and subtracting the common part, we can write down the final solution in the whole domain as

$$T(r,z,t) = -\frac{d}{c} + \frac{dJ_0(\sqrt{\frac{c}{a}}r)}{cJ_0(\sqrt{\frac{c}{a}})} + \sum_{n=1}^{\infty} \bar{D}_n J_0(\bar{\delta}_n r)\exp(-\bar{\lambda}_n^2 t) + \int_0^{\infty} (f_1(\omega,t) + f_2(\omega,t))\sin\left(\frac{1-z}{\sqrt{b}}\omega\right)\,\mathrm{d}\omega. \tag{66}$$

4 Analysis for the pressure hold time $t_{\rm p} < t \le t_{\rm f}$

For $t \ge t_{\rm p}$, heating no longer occurs due to the increase in pressure, and hence the right-hand side of the PDE in system (16) is zero. Rescaling time as $\zeta = t - t_{\rm p}$, we have

$$\begin{cases} \dfrac{\partial T}{\partial \zeta} - a\dfrac{1}{r}\dfrac{\partial}{\partial r}\left(r\dfrac{\partial T}{\partial r}\right) - b\dfrac{\partial^2 T}{\partial z^2} = 0 & \text{in} \quad (0,1)\times(0,1)\times(0, t_{\rm f}-t_{\rm p}), \\ \dfrac{\partial T}{\partial r} = 0 & \text{on} \quad r = 0, \\ T = 0 & \text{on} \quad r = 1, \\ \dfrac{\partial T}{\partial z} = 0 & \text{on} \quad z = 0, \\ T = 0 & \text{on} \quad z = 1, \\ T = T_{\rm up}(r,z) & \text{at} \quad \zeta = 0, \end{cases} \tag{67}$$

where $T_{\rm up}(r,z)$ is the solution $T(r,z,t)$ of the problem (solved in Section 3.1) in the time interval $0 < t < t_{\rm p}$, at time $t = t_{\rm p}$, namely

$$T_{\rm up}(r,z) = \frac{d}{c}\left(\frac{\cos(\gamma z)}{\cos\gamma} - 1\right) + \sum_{p=1}^{\infty} A_p J_0(\alpha_p r)\cos(\nu_p z) + \sum_{n=1}^{\infty}\sum_{m=1}^{\infty} D_{mn} J_0(\delta_n r)\cos(\nu_m z)\exp(-\lambda_{mn}^2 t_{\rm p}). \tag{68}$$

We now describe how to extend the analysis given above, for the pressure up time, to the system in the pressure hold time.

4.1 Exact solution

The analysis here is similar to that described in Section 3.1, but is in fact simpler because the right-hand side of the PDE is zero and so the problem is already homogeneous. Thus the solution is

$$T(r,z,t) = \sum_{j=1}^{\infty}\sum_{k=1}^{\infty} E_{kj} J_0(\eta_j r)\cos(\nu_k z)\exp(-\varphi_{kj}^2 (t - t_{\rm p})), \tag{69}$$

where $\eta_j \in \mathbb{R}$ satisfy $J_0(\eta_j) = 0$, $\nu_k = (k - 1/2)\pi$, and $\varphi_{kj} = \sqrt{a\eta_j^2 + b\nu_k^2}$. To determine coefficients E_{kj} we use the initial condition in (67), where $T_{\rm up}$ is defined in (68). Thus, after integrating and applying the orthogonality conditions, we have

$$E_{kj} = \frac{2\int_0^1\int_0^1 T_{\rm up}(r,z) r J_0(\eta_j r)\cos(\nu_k z)\,{\rm d}r\,{\rm d}z}{\int_0^1 r J_0^2(\eta_j r)\,{\rm d}r}. \tag{70}$$

4.2 Approximation ignoring the z-dependence

Again, assuming $b << a$, we ignore the z-dependence in (67) and solve the 1D problem, which is

$$\begin{cases} \dfrac{\partial T}{\partial \zeta} - a\dfrac{1}{r}\dfrac{\partial}{\partial r}\left(r\dfrac{\partial T}{\partial r}\right) = 0 & \text{in} \quad (0,1)\times(0, t_{\rm f}-t_{\rm p}), \\ \dfrac{\partial T}{\partial r} = 0 & \text{on} \quad r = 0, \\ T = 0 & \text{on} \quad r = 1, \\ T = T_{\rm up}(r) & \text{at} \quad \zeta = 0, \end{cases} \tag{71}$$

where $T_{\rm up}(r)$ is the 1D pressure up solution given in Section 3.2.1 at $t = t_{\rm p}$, i.e.

$$T_{\rm up}(r) = -\frac{d}{c} + \frac{dJ_0(\sqrt{\frac{c}{a}}r)}{cJ_0(\sqrt{\frac{c}{a}})} + \sum_{n=1}^{\infty} \bar{D}_n J_0(\bar{\delta}_n r) \exp(-\bar{\lambda}_n^2 t_{\rm p}). \tag{72}$$

A separation of variables solution to system (71) can be found using the same analysis as in previous sections. Thus we simply quote the solution as

$$T(r,t) = \sum_{j=1}^{\infty} \bar{E}_j J_0(\bar{\eta}_j r) \exp(-\bar{\varphi}_j^2 (t - t_{\rm p})), \tag{73}$$

where $\bar{\eta}_j \in \mathbb{R}$ satisfy $J_0(\bar{\eta}_j) = 0$, and $\bar{\varphi}_j = \sqrt{a}\ \bar{\eta}_j$. To determine coefficients $\bar{E}_j$ we use the initial condition in (71). After integrating and applying the orthogonality condition, we have

$$\bar{E}_j = \frac{\int_0^1 T_{\rm up}(r) J_0(\bar{\eta}_j r) r \, {\rm d}r}{\int_0^1 r J_0^2(\bar{\eta}_j r) \, {\rm d}r}, \tag{74}$$

where $T_{\rm up}(r)$ is defined in (72).

A boundary layer solution in 1D, like the one described in Section 3.2.2, was not given here because a boundary layer near $r = 1$ is no longer expected. This is due to the fact that the PDE in (71) has a right-hand side equal to zero, so now the a term becomes more important than in the pressure up time, where the c and d terms were dominant.

4.3 Approximation including the z-dependence

Following Section 3.3 we consider a boundary layer analysis near $z = 1$ by setting $z = 1 - \sqrt{b}\bar{z}$ and denote $T_{\rm in}(r, \bar{z}, \zeta)$ as the inner solution. Then system (67) becomes

$$\begin{cases} \dfrac{\partial T_{\rm in}}{\partial \zeta} - a\dfrac{1}{r}\dfrac{\partial}{\partial r}\left(r\dfrac{\partial T_{\rm in}}{\partial r}\right) - \dfrac{\partial^2 T_{\rm in}}{\partial \bar{z}^2} = 0 & \text{in} \quad (0,1)\times(0,\infty)\times(0, t_{\rm f} - t_{\rm p}), \\ \dfrac{\partial T_{\rm in}}{\partial r} = 0 & \text{on} \quad r = 0, \\ T_{\rm in} = 0 & \text{on} \quad r = 1, \\ T_{\rm in} \to T_{\rm out}(r,t) & \text{as} \quad \bar{z} \to \infty, \\ T_{\rm in} = 0 & \text{on} \quad \bar{z} = 0, \\ T = T_{\rm up}(r) & \text{at} \quad \zeta = 0, \end{cases} \tag{75}$$

where $T_{\rm up}(r)$ is given in (72), and $T_{\rm out}(r,t)$ in (73). Following the same setps as in Section 3.3 the solution is found to be

$$T(r,z,t) = T_{\rm out}(r,t) + \sum_{j=1}^{\infty} \int_0^{\infty} \frac{2\omega}{\pi} \bar{E}_j J_0(\bar{\eta}_j r) \frac{\left[\exp(-\bar{\varphi}_j^2 \zeta) - \exp(-\omega^2 \zeta)\right]}{\bar{\varphi}_j^2 - \omega^2} \sin\left(\frac{1-z}{\sqrt{b}}\omega\right). \tag{76}$$

5 Numerical tests

For the numerical tests we consider similar dimensions to the ones of the pilot unit (ACB GEC Alsthom, Nantes, France), used by other authors [5, 9], but we ignore the pressurizing fluid domain and the rubber cap and focus on the food and surrounding steel domains. The dimensions for these

are given in Table 1. Following [5, 9] we have chosen tylose (a food simile) as an example of solid type food. In order to reduce computational complexity, and following [5], we assume that the thermo-physical properties of the food sample are constant (and set them to their mean value in the range of temperature and pressure considered in the process). The thermo-physical properties of the steel remain constant during the whole process.

The initial temperature is $T_0 = 313$ K $= 39.85°$C in both the food and the steel, and the pressure is linearly increased during the first 183 seconds until it reaches 360 MPa. Then the pressure is maintained constant until the final time (900 seconds) is reached. Thus, the pressure generated by the equipment satisfies $P(0) = 0$ and

$$\frac{\mathrm{d}P}{\mathrm{d}t}(t) = \begin{cases} \dfrac{360}{183} \cdot 10^6 \text{ Pa s}^{-1}, & 0 < t \leq 183, \\ 0 \text{ Pa s}^{-1}, & 183 < t < 900. \end{cases} \tag{77}$$

ρ_{F}	1006	ρ_{S}	7833	$C_{p\mathrm{F}}$	3780	$C_{p\mathrm{S}}$	465
k_{F}	0.49	k_{S}	55	β_{F}	$4.217 \cdot 10^{-4}$	γ	$360 \cdot 10^6$
L	0.045	L_2	0.09	H	0.091	H_2	0.327
T_0	313	T_{r}	292.3	t_{p}	183	t_{f}	900

Table 1: Parameter values for numerical simulations. The food properties are those of tylose. Data is obtained from [2, 5, 8].

Following the procedure described in Section 2.2, and considering the values given in Table 1, the scales used to non-dimensionalise the variables are: $R = 0.045$ m, $Z = 0.091$ m, $\Delta T = 20.7$ K and $\tau = 325$ s. The values of a, b, c and d are shown in Table 2 (we point out that they satisfy the assumptions considered in the previous sections). The non-dimensional initial condition is $T_0^* = 1$.

	a	b	c	d
$\hat{\Omega}_{\mathrm{F}}$	0.02	0.005	0.07	1
$\hat{\Omega}_{\mathrm{S}}$	2.423	0.593	0	0

Table 2: Non-dimensional parameter values for system (10).

In Sections 3 and 4 we have given an exact solution and several simplifications to our problem. In order to check the validity of such simplifications we compare them to the reference models, which are considered to be the exact solution given in Section 3.1 for the pressure up time, and the one given in Section 4.1 for the pressure hold. Also a numerical solution in both 1D (using radial coordinates) and 2D (using cylindrical coordinates) is calculated using the FEM solver COMSOL Multiphysics 3.5a. In [5, 9] similar, although more complex, models were solved numerically using this commercial software, and validated by comparing to experimental data. Our model is a simplification of ones proposed in those papers, and not based on a real experiment, so we choose a numerical solution solved with COMSOL rather than a comparison to experimental data.

All of our solutions were calculated using MATLAB 7.12.0.635 (R2011a) without requiring an FEM solver. For the separation of variables solutions, the transcendental equation $J_0(x) = 0$, which appears in Sections 3.1, 3.2.1, 4.1 and 4.2, was solved using this software, whose roots correspond to δ_n, $\bar{\delta}_n$, η_j, $\bar{\eta}_j$ for each section, respectively. Coefficients $\bar{D}_n$ and $\bar{E}_j$ that appear in equations (39)

and (74), respectively, were calculated using integration formulas for Bessel functions. Coefficients D_{mn} and E_{kj} in equations (33) and (70) were calculated using a double trapezoidal rule for for the sake of simplicity, although the same rules for Bessel functions plus some for trigonometric functions could have been used for calculating it directly, or any other quadrature rule could also be used. We truncated each infinite sum and took as many terms as necessary to obtain a solution which did not vary to 16 decimal places from the solution with one term less. Thus, for equations (31) and (38) we took $N = 20$ terms, and for (69) and (72), $J = 20$ terms. For equations (26), $P = 35$ terms, for (31), $M = 35$ terms and for (69), $K = 35$ terms.

For the boundary layer solutions described in Sections 3.2.2 and 3.3, in which there are a semi-infinite integrals (namely (54) and (66)) to calculate, we followed [7], where a method to approximate integrals of the form $\int_a^\infty f(x)\,\phi(x)\,\mathrm{d}x$ is proposed, with $\phi(x)$ being either $\sin(\omega x)$ or $\cos(\omega x)$ is proposed. The integral is approximated by a numerical integration over a finite domain (a, b), leaving a truncation error equal to the tail integration $\int_b^\infty f(x)\,\phi(x)\,\mathrm{d}x$, plus the discretization error. Luo and Shevchenko [7] describe a very simple end-point correction to approximate the tail integration, which reduces significantly the truncation error, and which we have used in our calculations.

5.1 Results

Figure 2 shows the dimensionless temperature profiles given by the models presented in Section 3 for pressure up time. We have plotted the results of the 2D models at a fixed time ($t = 0.12$ on the left, $t = 0.56 = t_\mathrm{p}$ on the right) for different heights and for all r. As can be seen for all heights $z \in (0, 0.95)$ the solution is almost the same, and also matches perfectly with the 1D results from Sections 3.2.1 and 3.2.2. Then for the rest of heights up to $z = 1$, where the boundary layer is, it is clear that the solutions differ from the 1D model for the points very close to the top right corner of the 2D domain. There is a slight difference between the boundary layer solution given in Section 3.3 and the exact solution given in Section 3.1, especially near $r = 1$. This is because in (60) we are ignoring the a term, and therefore no heat conduction in the r direction is taken into account in this solution. Including this term leads to a problem which is more difficult to solve than the original one, and so the approximation would no longer be a simplification.

Figure 3 shows the dimensionless temperature profiles given by the models presented in Section 4 for pressure hold time. In this case the plots are at times $t = 1.50$ on the left and $t = 2.76 = t_\mathrm{f}$ on the right. For all heights $z \in (0, 0.94)$ the solution is almost the same and again matches perfectly with the 1D results from Section 4.2. In this case, however, for the rest of height up until $z = 1$ which are in the boundary layer, the approximation proposed in Section 4.3 differs more from the exact solution given in Section 4.1 than in the pressure up time case. This is because the conduction term in the r direction was ignored again, and, because there is no source term for the pressure hold case, this difference is more noticeable. We remark again that this slight discrepancy is for points that are very close to the top of the 2D domain.

Looking at the results we can see that the temperature profiles inside the food can be very well approximated by the 1D solution at nearly all heights inside the machine, except those very near the top, where a boundary layer exists. We point out that these are the results for the upper half of the domain (after our simplification in Section 2.2) and therefore by symmetry the same results hold for the lower half of the machine, i.e. the temperature profile for all heights except those near the bottom boundary can be very well approximated by a 1D model.

6 Extension to third class boundary conditions

We now consider a model where only the food domain is included, and assume that there is heat exchange between the walls of the food domain and the outside. Hence now the boundary and initial

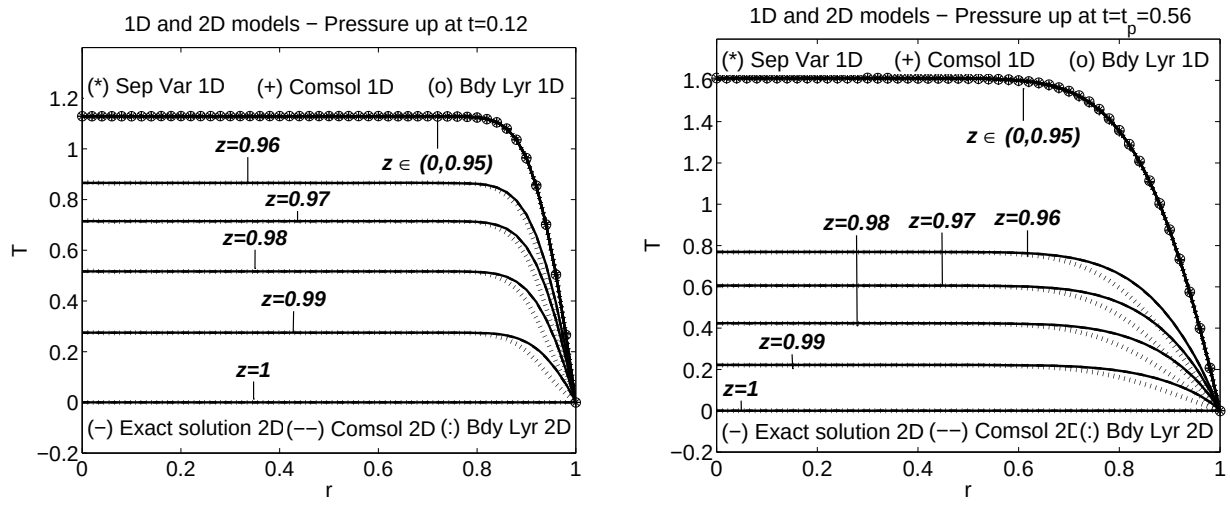

Figure 2: *Dimensionless temperature profiles calculated with different methods in 1D and 2D for pressure up at* $t = 0.12$ *(left) and* $t = t_{\mathrm{p}} = 0.56$ *(right).*

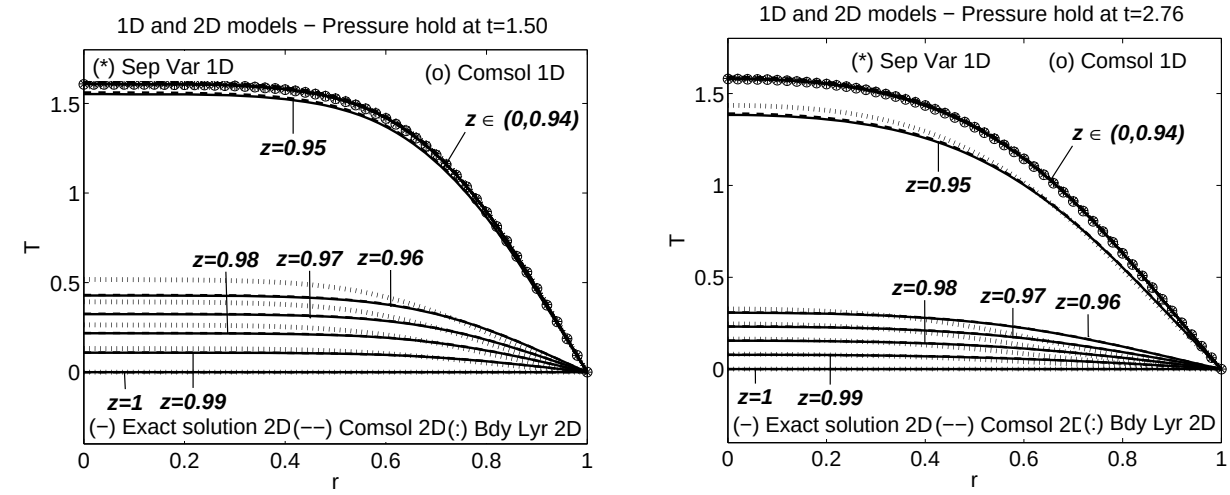

Figure 3: *Dimensionless temperature profiles calculated with different methods in 1D and 2D for pressure hold at* $t = 1.50$ *(left) and* $t = t_{\mathrm{f}} = 2.76$ *(right).*

conditions for (3) are

$$\begin{cases} \dfrac{\partial T}{\partial r} = 0 & \text{on} \quad \Gamma_{\text{sym}}, \\ k\dfrac{\partial T}{\partial \mathbf{n}} = h(T_{\text{r}} - T) & \text{on} \quad \Gamma_{\text{exc}} = \Gamma_{\text{F}} \setminus \Gamma_{\text{sym}}, \\ T = T_0 & \text{at} \quad t = 0, \end{cases} \tag{78}$$

where Γ_{F} is the boundary of Ω_{F}, h (W m^{-2} K^{-1}) is the heat transfer coefficient with the environment, and $\mathbf{n}$ is the outward unit normal vector on the boundary of the domain, Γ_{exc}.

Proceeding as in Section 2.2, we now have the following non-dimensional system to solve

$$\begin{cases} \dfrac{\partial T}{\partial t} - a\dfrac{1}{r}\dfrac{\partial}{\partial r}\left(r\dfrac{\partial T}{\partial r}\right) - b\dfrac{\partial^2 T}{\partial z^2} = (cT + d)\chi(t) & \text{in} \quad (0,1)\times(0,1)\times(0,t_{\text{f}}), \\ \dfrac{\partial T}{\partial r} = 0 & \text{on} \quad r = 0, \\ \epsilon_{\text{r}}\dfrac{\partial T}{\partial r} = -T & \text{on} \quad r = 1, \\ \dfrac{\partial T}{\partial z} = 0 & \text{on} \quad z = 0, \\ \epsilon_{\text{z}}\dfrac{\partial T}{\partial z} = -T & \text{on} \quad z = 1, \\ T = T_0^* & \text{at} \quad t = 0, \end{cases} \tag{79}$$

where $\epsilon_{\text{r}} = \frac{k}{hR}$ and $\epsilon_{\text{z}} = \frac{k}{hZ}$.

A similar analysis to that given for system (16), as described in Sections 3 and 4, can also be carried out for (79). Here we present only the results for the one dimensional approximation, ignoring the z-dependence for pressure up time.

6.1 Approximation ignoring the z-dependence for pressure up time

Following 3.2, if we assume that we are modelling a narrow and tall machine, and hence $b \ll a$, it is reasonable to ignore the z dependence in (79) and solve the 1D problem, which is given by

$$\begin{cases} \dfrac{\partial T}{\partial t} - a\dfrac{1}{r}\dfrac{\partial}{\partial r}\left(r\dfrac{\partial T}{\partial r}\right) = (cT + d) & \text{in} \quad (0,1)\times(0,t_{\text{p}}), \\ \dfrac{\partial T}{\partial r} = 0 & \text{on} \quad r = 0, \\ \epsilon_{\text{r}}\dfrac{\partial T}{\partial r} = -T & \text{on} \quad r = 1, \\ T = T_0^* & \text{at} \quad t = 0. \end{cases} \tag{80}$$

We now consider an exact and an approximate solution to this simplified system.

6.1.1 Separation of variables 1D

The analysis here is similar to that described in Section 3.2.1 but with a different boundary condition. To create a homogeneous problem we substitute $T(r,t) = u(r,t) + v(r)$ into (80). Then the problem

to solve for u is

$$\begin{cases} \dfrac{\partial u}{\partial t} = a\dfrac{1}{r}\dfrac{\partial}{\partial r}\left(r\dfrac{\partial u}{\partial r}\right) + cu & \text{in} \quad (0,1)\times(0,t_{\rm p}), \\ \dfrac{\partial u}{\partial r} = 0 & \text{on} \quad r=0, \\ \epsilon_{\rm r}\dfrac{\partial T}{\partial r} = -T & \text{on} \quad r=1, \\ u = T_0^* - v(r) & \text{at} \quad t=0, \end{cases} \tag{81}$$

whilst the problem for v is

$$0 = \frac{a}{r}\big(v'(r) + rv''(r)\big) + cv + d, \tag{82}$$

with $v'(0)=0$ and $\epsilon_{\rm r}v'(1) = -v(1)$. This has solution

$$v(r) = \frac{d}{c}\Big[\frac{J_0(\sqrt{\frac{c}{a}}r)}{J_0(\sqrt{\frac{c}{a}}) - \epsilon_{\rm r}\sqrt{\frac{c}{a}}J_1(\sqrt{\frac{c}{a}})} - 1\Big]. \tag{83}$$

A straightforward calculation gives the solution for u as

$$u(r,t) = \sum_{n=1}^{\infty} \bar{\bar{D}}_n J_0(\bar{\bar{\delta}}_n r)\exp(-\bar{\bar{\lambda}}_n^2 t), \tag{84}$$

where $\bar{\bar{\delta}}_n \in \mathbb{R}$ satisfy

$$\epsilon_{\rm r}\bar{\bar{\delta}}J_1(\bar{\bar{\delta}}_n) = J_0(\bar{\bar{\delta}}_n), \tag{85}$$

$\bar{\bar{\lambda}}_n = \sqrt{a\bar{\bar{\delta}}_n^2 - c}$ and coefficients $\bar{\bar{D}}_n$ are given by

$$\bar{\bar{D}}_n = \frac{2\int_0^1 \left(T_0^* - v(r)\right)\, rJ_0(\bar{\bar{\delta}}_n r)\,{\rm d}r}{\int_0^1 rJ_0^2(\bar{\bar{\delta}}_n r)\,{\rm d}r}, \tag{86}$$

with $v(r)$ defined in (83). Finally, the solution T is simply the sum of u and v.

6.1.2 Boundary layer in r

To consider a boundary layer in r we start with system (80). Analogously to Section 3.2.2 we assume $d = \mathcal{O}(1)$ and $b < a \ll 1$. Then ignoring the terms involving a and b, we again have at leading order the outer solution given by (42), i.e.

$$T(t) = -\frac{d}{c} + \left(T_0^* + \frac{d}{c}\right)\exp(ct). \tag{87}$$

It is clear that since solution (87) only depends on t it does satisfy the zero flux condition at $r=0$, but it obviously cannot satisfy the third class boundary condition at $r=1$. Therefore we consider a boundary layer near $r=1$. Following the exact steps as in Section 3.2.2, we introduce the boundary-layer coordinate given by (43), take $\delta = \sqrt{a}$ to bring out the correct balance in the equation, which at leading order is

$$\begin{cases} \dfrac{\partial T_{\rm in}}{\partial t} = \dfrac{\partial^2 T_{\rm in}}{\partial \bar{r}^2} - \sqrt{a}\dfrac{\partial T_{\rm in}}{\partial \bar{r}} + cT_{\rm in} + d & \text{in} \quad (0,\infty)\times(0,t_{\rm p}), \\ \dfrac{\partial T_{\rm in}}{\partial \bar{r}} = \dfrac{\delta}{\epsilon_{\rm r}}T_{\rm in} & \text{on} \quad \bar{r}=0, \\ T_{\rm in} \to T_{\rm out}(t) & \text{as} \quad \bar{r}\to\infty, \\ T_{\rm in} = T_0^* & \text{at} \quad t=0, \end{cases} \tag{88}$$

where $T_{\rm out}(t)$ is the outer solution given by (87). We define

$$T_{\rm in}(\bar{r},t) = T_{\rm out}(t) + \exp\left(\frac{\sqrt{a}\,\bar{r}}{2} + ct - \frac{at}{4}\right) G(\bar{r},t), \tag{89}$$

and so the system for G reduces to

$$\begin{cases} \dfrac{\partial G}{\partial t} = \dfrac{\partial^2 G}{\partial \bar{r}^2} & \text{in} \quad (0,\infty)\times(0,t_{\rm p}), \\ -\dfrac{\partial G}{\partial \bar{r}} + \alpha G = h(t) & \text{on} \quad \bar{r}=0, \\ G \to 0 & \text{as} \quad \bar{r}\to\infty, \\ G = 0 & \text{at} \quad t = 0, \end{cases} \tag{90}$$

where

$$\alpha = \frac{\sqrt{a}}{\epsilon_{\rm r}} - \frac{\sqrt{a}}{2}, \qquad h(t) = -\frac{\sqrt{a}}{\epsilon_{\rm r}} T_{\rm out}(t)\exp\left(-ct + at/4\right). \tag{91}$$

From [4] we know that (90) can be solved by taking the following integral transform

$$\hat{G}(\omega,t) = \int_0^\infty G(\bar{r},t)K(\omega,\bar{r})\,\mathrm{d}\bar{r}, \tag{92}$$

where $K(\omega,\bar{r})$ is the solution of

$$\begin{aligned} &\frac{\mathrm{d}^2 R(\bar{r})}{\mathrm{d}^2\bar{r}^2} + \omega^2 R(\bar{r}) = 0, \\ &\alpha R(\bar{r}) - \frac{\mathrm{d}R(\bar{r})}{\mathrm{d}\bar{r}} = 0 \qquad \text{on} \quad \bar{r}=0, \end{aligned} \tag{93}$$

namely

$$K(\omega,\bar{r}) = \sqrt{\frac{2}{\pi}}\Big[\frac{\omega\cos(\omega\bar{r}) + \alpha\sin(\omega\bar{r})}{\sqrt{\omega^2+\alpha^2}}\Big]. \tag{94}$$

Applying the integral transform (92) to the PDE in (90) gives

$$\int_0^\infty \frac{\partial G(\bar{r},t)}{\partial t} K(\omega,\bar{r})\,\mathrm{d}\bar{r} = \int_0^\infty \frac{\partial^2 G(\bar{r},t)}{\partial \bar{r}^2} K(\omega,\bar{r})\,\mathrm{d}\bar{r}. \tag{95}$$

Now

$$\int_0^\infty \frac{\partial^2 G(\bar{r},t)}{\partial \bar{r}^2} K(\omega,\bar{r})\,\mathrm{d}\bar{r} = -K\frac{\partial G}{\partial \bar{r}}\bigg|_{\bar{r}=0} + \frac{\mathrm{d}K}{\mathrm{d}\bar{r}} G\bigg|_{\bar{r}=0} - \omega^2 \int_0^\infty G(\bar{r},t)K(\omega,\bar{r})\,\mathrm{d}\bar{r}. \tag{96}$$

From (90) and (93) it follows that at $\bar{r}=0$

$$-K\frac{\partial G}{\partial \bar{r}} + \frac{\mathrm{d}K}{\mathrm{d}\bar{r}} G = -K(\alpha G - h(t)) + \alpha K G = h(t)K(\omega,0). \tag{97}$$

Hence

$$\int_0^\infty \frac{\partial^2 G(\bar{r},t)}{\partial \bar{r}^2} K(\omega,\bar{r})\,\mathrm{d}\bar{r} = -\omega^2\hat{G} + h(t)K(\omega,0) = -\omega^2\hat{G} + \sqrt{\frac{2}{\pi}}h(t)\frac{\omega}{\sqrt{\omega^2+\alpha^2}}, \tag{98}$$

and so the PDE in (90) becomes

$$\frac{\partial \hat{G}}{\partial t} + \omega^2\hat{G} = \sqrt{\frac{2}{\pi}}h(t)\frac{\omega}{\sqrt{\omega^2+\alpha^2}}, \tag{99}$$

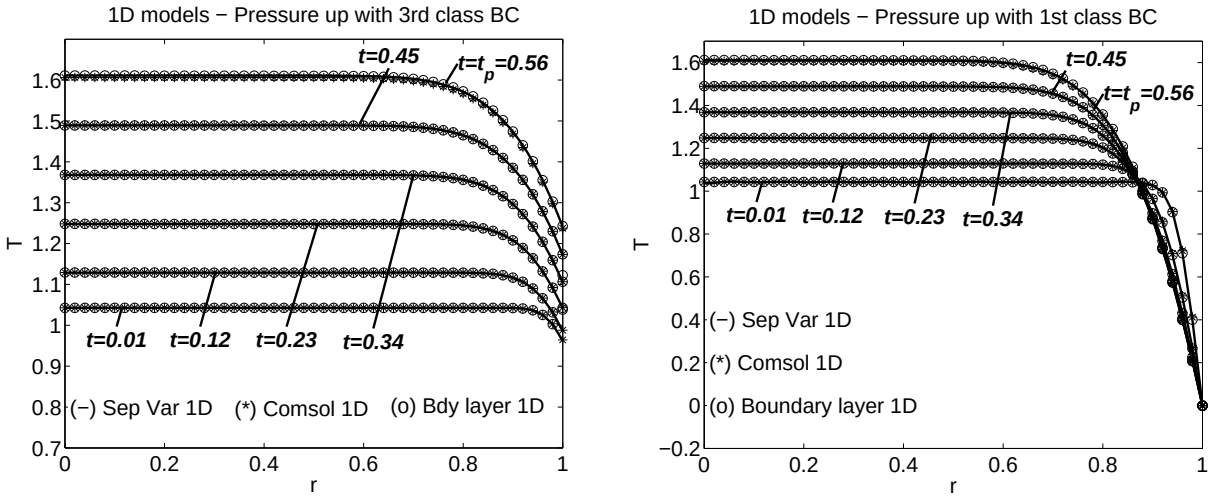

Figure 4: *Dimensionless temperature profiles calculated with different methods in 1D for the third class (left) and first class (right) boundary conditions.*

where $h(t)$ and α are defined in (91). The initial condition in (90) implies $\hat{G}(\omega, 0) = 0$, and so equation (99) has solution

$$\hat{G}(\omega,t) = \sqrt{\frac{2}{\pi}}\Big[\frac{\omega\sqrt{a}d}{\epsilon_{\rm r}c\sqrt{\omega^2+\alpha^2}}\frac{\exp(at/4-ct)-\exp(-\omega^2 t)}{\omega^2+a/4-c} - \frac{\omega\sqrt{a}(T_0^*+d/c)}{\epsilon_{\rm r}\sqrt{\omega^2+\alpha^2}}\frac{\exp(at/4)-\exp(-\omega^2 t)}{\omega^2+a/4}\Big], \tag{100}$$

after substituting $T_{\rm out}(t)$ from (87). Finally the solution for G (see [4]) is

$$G(\bar{r},t) = \sqrt{\frac{2}{\pi}}\Big[\int_0^\infty \hat{G}(\omega,t)\frac{\omega}{\sqrt{\omega^2+\alpha^2}}\cos(\omega\bar{r})\,{\rm d}\omega + \int_0^\infty \hat{G}(\omega,t)\frac{\alpha}{\sqrt{\omega^2+\alpha^2}}\sin(\omega\bar{r})\,{\rm d}\omega\Big], \tag{101}$$

and $T_{\rm in}(\bar{r},t)$ is given by (89). After adding the inner and outer solutions ans subtracting the common part, we can write down the final solution in the whole domain as

$$T(r,t) = -\frac{d}{c} + \left(T_0^* + \frac{d}{c}\right)\exp(ct) + \exp\left(\frac{1-r}{2} + ct - \frac{at}{4}\right) G\left(\frac{1-r}{\sqrt{a}}, t\right). \tag{102}$$

6.2 Results

We perform numerical tests for the problem with third class boundary conditions, using the same data and parameters as in Section 5. The heat transfer coefficient used in the tests is $h = 28$ W m^{-2} K^{-1}. Figure 4 shows the dimensionless temperature profiles that result from solving the pressure up time problem in 1D for boundary conditions of the third and first class (Sections 6.1 and 3.2, respectively). The temperature has been calculated using separation of variables in 1D (Sections 6.1.1 and 3.2.1, respectively), by a boundary layer in 1D approximation (Sections 6.1.2 and 3.2.2, respectively). Observe that both solutions match perfectly for all times, and also to the 1D COMSOL solution, which has been taken as a reference model. For the first class boundary conditions, an exact solution in 2D was given in Section 3.1. However, for the third class boundary condition we do not give all the possible solutions, as it is analogous to the ones derived throughout Sections 3 and 4, and we just concentrate on the 1D pressure up case.

7 Conclusions

We have presented heat transfer models for predicting temperature profiles inside a solid type food undergoing HP treatment. Two different kinds of boundary conditions have been considered depending on whether only the food holder is taken into account, or whether the surrounding steel is included. We have given a thorough analysis describing an exact 2D solution as well as several simplifications in both 2D and 1D. It has been shown that for the case of a tall and narrow HP machine, the temperature profile inside the food is very well approximated by a 1D model, except at points very close to the top and bottom boundaries. The reduction to 1D is extremely useful from a computational point of view because optimisation of these processes is easier, thus leading to faster simulations. In addition, the simplified model can help to calculate thermo-physical properties as a function of pressure, via inverse problems, which is an increasing need nowadays for food technologists. From an experimental point of view, results can also be used to determine where to place the thermocouples inside the food sample in order to measure the temperature experimentally. Finally, we point out that the solutions given here do not require the use of a "black-box" FEM solver and our approximations allow us to qualitatively describe the physical features involved

Acknowledgments

This work was carried out thanks to the financial support of the Spanish "Ministry of Science and Innovation" under projects MTM2008-04621, MTM2011-22658; the research group MOMAT (Ref. 910480) supported by "Banco Santander" and "Universidad Complutense de Madrid"; the "Comunidad de Madrid" and "European Social Fund" through project S2009/PPQ-1551. This publication was also based on work supported in part by the "Programa de Visitantes Distinguidos - Grupo Santander: Doctores y Tecnólogos". Also, SLM acknowledges the support of MACSI, the Mathematics Applications Consortium for Science and Industry (`www.macsi.ul.ie`), funded by the Science Foundation Ireland Mathematics Initiative Grant 06/MI/005.

References

[1] J. C. Cheftel. Review: high-pressure, microbial inactivation and food preservation. *Food Sci. Tech. Int.*, 1(2-3): 75–90, 1995.

[2] A. C. Cleland and R. L. Earle. Assessment of freezing time prediction methods. *J. Food Sci.*, 49: 1034–1042, 1995.

[3] S. Denys, L. R. Ludikhuyze, A. M. Van Loey, and M. E. Hendrickx. Modeling conductive heat transfer and process uniformity during batch high-pressure processing of foods. *Biotechnol. Prog.*, 16: 92–101, 2000.

[4] M. Necati Őzisik. *Boundary Value Problems of Heat Conduction.* Dover Publications Inc., New York, 1968.

[5] J. A. Infante, B. Ivorra, A. M. Ramos, and J. M. Rey. On the modelling and simulation of high pressure processes and inactivation of enzymes in food engineering. *Math. Models Methods Appl. Sci.*, 19(12): 2203–2229, 2009.

[6] K. Knoerzer, P. Juliano, S. Gladman, C. Versteeg, and P. J. Fryer. A computational model for temperature and sterility distributions in a pilot-scale high-pressure high-temperature process. *AIChE Journal*, 53(11): 2996–3010, 2007.

[7] X. Luo and P. V. Schevchenko. A short tale of long tail integration. *Numerical Algorithms*, 56:577, 2011.

[8] L. Otero, A. Ousegui, B. Guignon, A. Le Bail, and P. D. Sanz. Evaluation of the thermophysical properties of tylose gel under pressure in the phase change domain. *Food Hydrocolloids*, 20: 449–460, 2006.

[9] L. Otero, A. M. Ramos, C. de Elvira, and P. D. Sanz. A model to design high pressure processes towards a uniform temperature distribution. *J. Food Engng*, 78: 1463–1470, 2007.

[10] L. Otero and P. D. Sanz. Modelling heat transfer in high pressure food processing: a review. *Innovative Food Sci. Emerging Tech.*, 4: 121–134, 2003.

[11] Q. Tuan Pham. Modelling heat and mass transfer in frozen foods: a review. *Int. J. Refrigeration*, 29: 876–888, 2006.

[12] J. P. P. M. Smelt. Recent advances in the microbiology of high pressure processing. *Trends Food Sci. Tech.*, 9: 152–158, 1998.

[13] N. A. S. Smith, S. S. L. Peppin, and A. M. Ramos. Generalized enthalpy model of a high-pressure shift freezing process. *Proc. Roy. Soc. A*, 2012. doi=10.1098/rspa.2011.0622.

PREPUBLICACIONES DEL DEPARTAMENTO
DE MATEMÁTICA APLICADA
UNIVERSIDAD COMPLUTENSE DE MADRID
MA-UCM 2011

1. APPROXIMATING TRAVELLING WAVES BY EQUILIBRIA OF NON LOCAL EQUATIONS, J. M. Arrieta, M. López-Fernández and E. Zuazua.

2. INFINITELY MANY STABILITY SWITCHES IN A PROBLEM WITH SUBLINEAR OSCILLATORY BOUNDARY CONDITIONS, A. Castro and R. Pardo

3. THIN DOMAINS WITH EXTREMELY HIGH OSCILLATORY BOUNDARIES, J́. M. Arrieta and M. C. Pereira

4. FROM NEWTON EQUATION TO FRACTIONAL DIFFUSION AND WAVE EQUATIONS, L. Váquez

5. EL CÁLCULO FRACCIONARIO COMO INSTRUMENTO DE MODELIZACIÓN, L. Váquez and M. P. Velasco

6. THE TANGENTIAL VARIATION OF A LOCALIZED FLUX-TYPE EIGENVALUE PROBLEM, R. Pardo, A. L. Pereira and J. C. Sabina de Lis

7. IDENTIFICATION OF A HEAT TRANSFER COEFFICIENT DEPENDING ON PRESSURE AND TEMPERATURE, A. Fraguela, J. A. Infante, Á. M. Ramos and J. M. Rey

8. A NOTE ON THE LIOUVILLE METHOD APPLIED TO ELLIPTIC EVENTUALLY DEGENERATE FULLY NONLINEAR EQUATIONS GOVERNED BY THE PUCCI OPERATORS AND THE KELLER–OSSERMAN CONDITION, G. Díaz

9. RESONANT SOLUTIONS AND TURNING POINTS IN AN ELLIPTIC PROBLEM WITH OSCILLATORY BOUNDARY CONDITIONS, A. Castro and R. Pardo

10. BE-FAST: A SPATIAL MODEL FOR STUDYING CLASSICAL SWINE FEVER VIRUS SPREAD BETWEEN AND WITHIN FARMS. DESCRIPTION AND VALIDATION. B. Ivorra B. Martínez-López, A. M. Ramos and J.M. Sánchez-Vizcaíno.

11. FRACTIONAL HEAT EQUATION AND THE SECOND LAW OF THERMODYNAMICS, L. Vázquez , J. J. Trujillo and M. P. Velasco

12. LINEAR AND SEMILINEAR HIGHER ORDER PARABOLIC EQUATIONS IN R^N, J. Cholewa and A. Rodríguez Bernal

13. DISSIPATIVE MECHANISM OF A SEMILINEAR HIGHER ORDER PARABOLIC EQUATION IN R^N, J. Cholewa and A. Rodríguez Bernal

14. DYNAMIC BOUNDARY CONDITIONS AS A SINGULAR LIMIT OF PARABOLIC PROBLEMS WITH TERMS CONCENTRATING AT THE BOUNDARY, A. Jiménez-Casas and A. Rodríguez Bernal

15. DISEÑO DE UN MODELO ECONÓMICO Y DE PLANES DE CONTROL PARA UNA EPIDEMIA DE PESTE PORCINA CLÁSICA, E. Fernández Carrión, B. Ivorra, A. M. Ramos, B. Martínez-López, Sánchez-Vizcaíno.

16. BIOREACTOR SHAPE OPTIMIZATION. MODELING, SIMULATION, AND SHAPE OPTIMIZATION OF A SIMPLE BIOREACTOR FOR WATER TREATMENT, J. M. Bello Rivas, B. Ivorra, A. M. Ramos, J. Harmand and A. Rapaport

17. THE PROBABILISTIC BROSAMLER FORMULA FOR SOME NONLINEAR NEUMANN BOUNDARY VALUE PROBLEMS GOVERNED BY ELLIPTIC POSSIBLY DEGENERATE OPERATORS, G. Díaz

PREPUBLICACIONES DEL DEPARTAMENTO
DE MATEMÁTICA APLICADA
UNIVERSIDAD COMPLUTENSE DE MADRID
MA-UCM 2012

1. ON THE CAHN-HILLIARD EQUATION IN H^1(R^N), J. Cholewa and A. Rodríguez Bernal

2. GENERALIZED ENTHALPY MODEL OF A HIGH PRESSURE SHIFT FREEZING PROCESS, N. A. S. Smith, S. S. L. Peppin and A. M. Ramos

3. 2D AND 3D MODELING AND OPTIMIZATION FOR THE DESIGN OF A FAST HYDRODYNAMIC FOCUSING MICROFLUIDIC MIXER, B. Ivorra, J. L. Redondo, J. G. Santiago, P.M. Ortigosa and A. M. Ramos

4. SMOOTHING AND PERTURBATION FOR SOME FOURTH ORDER LINEAR PARABOLIC EQUATIONS IN R^N, C. Quesada and A. Rodríguez-Bernal

5. NONLINEAR BALANCE AND ASYMPTOTIC BEHAVIOR OF SUPERCRITICAL REACTION-DIFFUSION EQUATIONS WITH NONLINEAR BOUNDARY CONDITIONS, A. Rodríguez-Bernal and A. Vidal-López

6. NAVIGATION IN TIME-EVOLVING ENVIRONMENTS BASED ON COMPACT INTERNAL REPRESENTATION: EXPERIMENTAL MODEL, J. A. Villacorta-Atienza and V.A. Makarov

7. ARBITRAGE CONDITIONS WITH NO SHORT SELLING, G. E. Oleaga

8. THEORY OF INTERMITTENCY APPLIED TO CLASSICAL PATHOLOGICAL CASES, E. del Rio, S. Elaskar, and V. A. Makarov

9. ANALYSIS AND SIMPLIFICATION OF A MATHEMATICAL MODEL FOR HIGH-PRESSURE FOOD PROCESSES, N. A. S. Smith, S. L. Mitchell and A. M. Ramos